Confined Brownian motion

Luc P. Faucheux and Albert J. Libchaber*
Physics Department, Princeton University, Princeton, New Jersey 08544
(Received 7 October 1993; revised manuscript received 30 March 1994)

We present microscopic observations of the diffusion in water of micrometer-sized spheres confined between two walls. Deviations from the Stokes-Einstein law are observed, which for different bead diameters and different separations between the walls depend on a single dimensionless parameter. We compare numerical predictions with the experimental values.

PACS number(s): 51.20.+d, 05.40.+j, 66.10.Cb

I. INTRODUCTION

The diffusion coefficient D_0 of spherical particles of radius r in a fluid of viscosity η_0 at temperature T is given by the Stokes-Einstein formula [1]

$$D_0=(k_B T)/(6\pi\eta_0 r) . \quad (1)$$

It is there assumed that the velocity field of the surrounding fluid goes to zero at the particle surface and infinitely far from the particle.

Deviations from this law in normal liquids have already been observed, always due to a boundary at a finite distance from the bead. It may be the glass walls of a cell [2–4] or other beads [5,6]. A change in the material properties of the fluid around the bead in glass-forming liquids can also be treated as an effective boundary [7]. In any case, the Stokes-Einstein formula can be generalized by defining an effective viscosity (and hence an effective diffusivity) function of the bead diameter, position, and bead volume fraction.

We present in this paper a visualization using a microscope of a Brownian particle diffusing between two glass plates. Previous works used light correlation techniques. The diffusion coefficient is measured in our experiment from the observation of a single bead. From the horizontal projection of the Brownian trajectories, digitized and stored in real time, we extract the diffusion coefficient D for motions parallel to the glass plate. It deviates from the bulk value D_0 by as much as one third. The deviations are described by a continuous function of a dimensionless position parameter. We then compare our experimental results with analytic solutions [8]. As we do not record the vertical excursions of the bread inside the sample, we must average the analytical expressions over the vertical axis.

In Sec. II we describe the experimental setup and the sample preparation. We discuss the averaging process over many bead trajectories to extract the diffusion coefficient. We introduce a dimensionless position parameter γ. The deviation of the diffusivity from the bulk value is a function of γ.

In Sec. III, we review the analytical form of the diffusion coefficient for a bead close to a wall. We estimate the effective diffusion coefficient by averaging along the vertical axis. We finally discuss the generalization of Fick's law when the diffusion coefficient is spatially varying.

II. DEVIATION FROM THE STOKES-EINSTEIN LAW

In this section, we describe the experimental setup and present how we deduce the diffusion coefficients from the measurements. We then introduce a simple model explaining the deviation from the bulk value for diffusion.

A. Experimental setup

Samples were prepared as follows: Silica and latex spheres [9] were diluted and sonicated in ultrapure water [10]. The volume fraction was around 10^{-5} so that typically only a few beads were seen in the field of view (50×50 μm^2). We avoid any hydrodynamic interaction between beads by using such a low volume fraction. Several monodispersed suspensions of beads between 1 and 3 μm in diameter were used.

Fine wires [11] with diameters from 6 to 100 μm were used as spacers between a microscope slide [12] and a coverslip [13], previously cleaned using a Nitrogene gas ionizing gun [14]. We used a coverslip because of the short working distance of the microscope objective. In order to avoid fluid flow, the cell was first partially sealed using fast epoxy [15], then filled with the beads in solution and completely sealed with fast epoxy. Beads did not stick to each other or to the glass plates for at least a day, before pollution of the water by the fast epoxy occurred. Typical experiments lasted 2 h.

The sample was then placed on the stage of an inverted microscope [16] equipped with an oil immersed objective [17] of magnification $100\times$, as shown in Fig. 1. The bead was observed with a CCD camera [18] coupled to the microscope via coupling lenses [19] of additional magnification of $2.5\times$ and $6.7\times$. The video signal was processed in real time by a computer [20]. The computer recorded the X and Y coordinates of the center of mass of the bead, the X and Y axis being defined in Fig. 1. The displacement of the bead in the vertical direction was not

*Also at NEC Research Institute, 4 Independence Way, Princeton, NJ 08540.

 ©1994 The American Physical Society

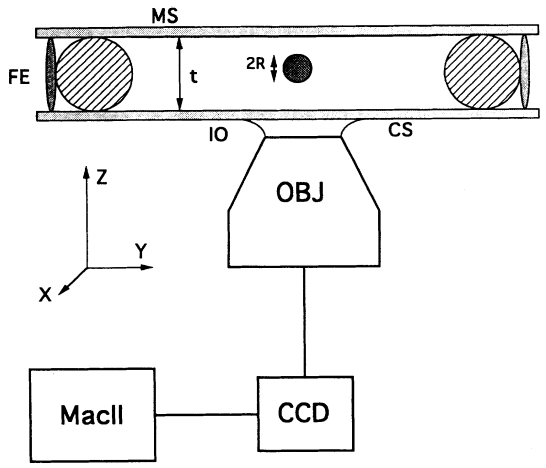

FIG. 1. The experimental setup: beads of diameter $2r$ are suspended in water between a microscope slide (MS) and a cover slip (CS), separated by wires of diameter t. The cell is sealed with fast epoxy (FE). The objective (OBJ) is coupled to the sample by optically index matched immersion oil (IO). The CCD camera digitizes the image which is transmitted to a MacII computer.

recorded. Constant adjustment of the focus was needed during the experiment for the lightest beads (1 μm diameter in latex).

Let us now discuss briefly the sampling rate and the total recording time. As we processed the video signal in real time, the larger the bead appears on the computer screen, the longer the processing time required and the slower the sampling rate. Depending upon the diameter of the bead and the optical magnification, the sampling rate ranged between 0.05 s and 0.2 s. This rate was, however, well adjusted for our experiment: the diffusion coefficient being of the order of 1 $\mu m^2/s$, the bead moves by only a fraction of its diameter (≈ 1 μm) between two successive recordings. We recorded 2048 successive positions of the bead, which correspond to a time series of about 3 min. This time was short enough so that the bead would not escape outside the field of view. We rejected any experiment where more than one bead was present within the field of view. Typically 12 time series were used for each sample. This corresponds to half an hour of recording for a given sample (given the separation between the plates, bead density, and bead diameter). We checked that the number of time series was large enough to get a good measurement of the diffusion coefficient, using the following averaging procedure.

B. Diffusion coefficients

From the X and Y coordinates of the bead as a function of time, we recover the projection of the bead trajectory onto the X-Y plane (see Fig. 2). We then plot the square of the distance from the bead's original position, $R^2(t)$, as a function of time (thin dotted line in Fig. 3). The diffusion coefficient is proportional to the slope of the statistical average (i.e., over many beads) of this quantity. To improve our statistics, we divide each trajectory into shorter ones. As the Brownian motion is stochastic, the

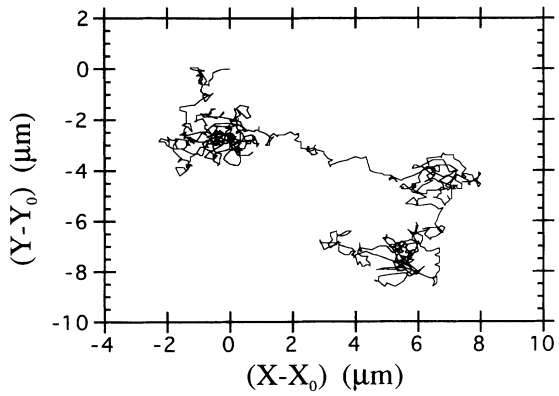

FIG. 2. The projection onto the X-Y plane of the trajectory of a 1.5 μm diameter latex bead inside a 25 μm thick sample (sample 17 in Table I). Recording time 70 s.

short trajectories are independent from each other. We then average over all paths of the same duration in all the fields corresponding to a given sample. The result (thick dotted line in Fig. 3) shows the expected linear dependence for short times. The statistics are evidently better at short times, where more trajectories can be averaged over. We define the diffusion coefficient D for motions parallel to the glass plates, as the slope of the linear fit is divided by four.

The ratio D/D_0 is calculated for all the samples (see Table I). The bulk diffusion coefficient D_0 is computed from Eq. (1). D/D_0 shows a severe deviation from the Stokes-Einstein law (as much as $\frac{1}{3}$).

C. A simple model

We present here the effect of walls on the diffusion of a bead and introduce a dimensionless position parameter γ such that all the measurements of D/D_0 fit on a smooth curve as a function of γ.

Let us consider a bead of radius r at a distance z from a

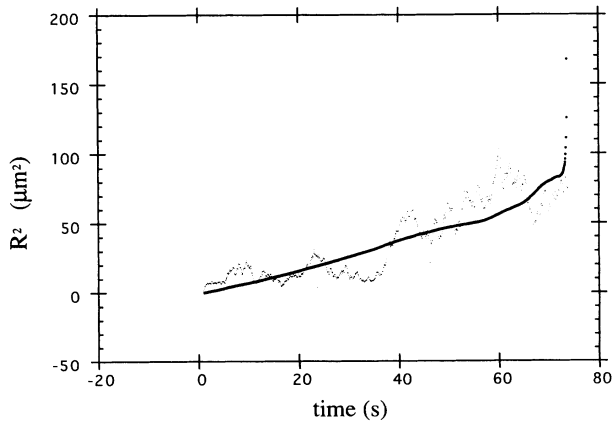

FIG. 3. Thin dotted line: the square of the distance from the bead original position (X_0, Y_0) in μm^2 as a function of time in s for a 1.5 μm diameter latex bead in a 25 μm thick sample (sample 17 in Table I). Thick line: the result of the averaging procedure described in the text.

TABLE I. The different samples are sorted with increasing value of γ. The Boltzmann length scale is computed from Eq. (4). The vertical equilibrium displacement from the bottom plate h is computed using Eq. (6). The dimensionless parameter γ is computed from Eq. (2). D(expt) is the measured diffusivity. D_0 is the bulk value from Eq. (1). D (theor) is computed from Eq. (14).

Sample No.	Bead diameter (μm)	Bead density	L (μm)	Sample thickness (μm)	h (μm)	γ	D/D_0 (expt)	D/D_0 (theor)
1	2.5	2.1	0.05	6	1.3	0.04	0.32	0.31
2	2.5	2.1	0.05	25	1.3	0.04	0.36	0.32
3	2.5	2.1	0.05	100	1.3	0.04	0.36	0.32
4	2.5	2.1	0.05	1000	1.3	0.04	0.36	0.32
5	3.5	1.05	0.37	12	2.1	0.2	0.4	0.36
6	3.5	1.05	0.37	50	2.1	0.2	0.41	0.38
7	3	1.05	0.60	12	2.1	0.4	0.35	0.39
8	2.5	1.05	1.03	12	2.3	0.8	0.38	0.42
9	2	1.05	2.02	6	2.4	1.4	0.45	0.48
10	1	2.1	0.73	6	1.2	1.4	0.41	0.36
11	1	2.1	0.73	25	1.2	1.4	0.42	0.36
12	1	2.1	0.73	100	1.2	1.4	0.56	0.54
13	2	1.05	2.02	12	2.9	1.9	0.61	0.56
14	1.5	1.05	4.8	6	2.6	2.5	0.52	0.54
15	1.5	1.05	4.8	12	4.2	4.6	0.78	0.67
16	1	1.05	16.1	6	2.8	4.6	0.71	0.58
17	1.5	1.05	4.78	25	5.3	6.1	0.81	0.76
18	1	1.05	16.1	12	5.2	9.4	0.87	0.82
19	1	1.05	16.1	25	9	17	0.82	0.85
20	1	1.05	16.1	50	12	23	0.89	0.92

glass plate, moving parallel to the glass plate. The deviation of the diffusion coefficient from D_0 is a hydrodynamic effect: the closer the bead is to a wall, where the velocity field has to go to zero, the bigger the drag force on a particle moving parallel to this wall [8,19,21]. A simple reason is that the closer boundary allows less space for the surrounding fluid to be transported around the sphere as this one moves [22]. In order to keep the usual formulation of the drag force ($-6\pi\eta_0 rv$, where v is the bead velocity), we replace η_0 by an effective viscosity η. The effective diffusivity is then $D=D_0(\eta/\eta_0)^{-1}$. It decreases as the bead gets closer to the wall. Since the hydrodynamic equations for the velocity field in the low Reynolds number limit do not contain any natural length scale, D has to be a function of a dimensionless parameter. In the case of a bead close to a wall, the only dimensionless parameter available is z/r. It is, however, more convenient to use $\gamma=(z-r)/r$. The effective diffusivity then increases up to its bulk value D_0 as γ goes from zero to infinity.

Since we do not keep track of the vertical Brownian excursions of the bead, the effective diffusivity D is averaged over the Z axis. Thus, one can replace in the previous discussion z by h, the average vertical position of the bead. The position parameter γ is then

$$\gamma=\left[\frac{h-r}{r}\right] . \tag{2}$$

The average vertical position h is computed using the usual Boltzmann density profile $P_B(z)$ of beads of radius r and density ρ in a fluid of density ρ_0 and temperature T, confined between the planes ($z=0$) and ($z=t$) in a gravitational field of acceleration g:

$$P_B(z)=\left[\frac{1}{L}\right]\left[\frac{e^{-z/L}}{e^{-r/L}-e^{(r-t)/L}}\right] , \tag{3}$$

where L is the characteristic Boltzmann length scale

$$L=k_BT/\Delta mg \tag{4}$$

and where

$$\Delta m=\tfrac{4}{3}\pi r^3(\rho-\rho_0) . \tag{5}$$

L is to be compared with the two length scales r and t. If L is smaller than the radius r, the bead sediments to the bottom plate. If L is larger than the sample thickness t, the bead explores vertically the whole sample. The average vertical position h is thus

$$h=\int_r^{t-r} zP_B(z)dz$$
$$=\frac{e^{-r/L}[rL+L^2]-e^{(r-t)/L}[(t-r)L+L^2]}{L(e^{-r/L}-e^{(r-t)/L})} . \tag{6}$$

Since two walls are present, one should consider $\gamma=(h-r)/r$ and $\gamma'=(t-h+r)/r$ for the bottom and top plates, respectively. However, since in our experiment most of the beads tend to sediment close to the bottom plate, it is a good approximation to consider only the effect of the bottom plate, and to look at the dependence of D/D_0 on γ. Note that γ still depends on the thickness t via the equilibrium vertical position h. The table gives the value of r, ρ, t, L, h, γ, and D/D_0 for each sample.

If γ is indeed the right parameter to describe the devia-

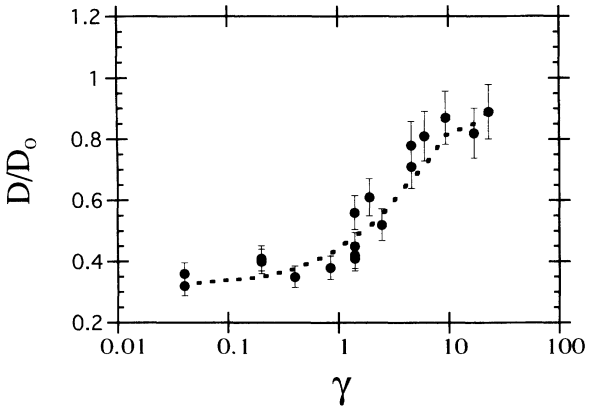

FIG. 4. The experimental ratio D/D_0 as a function of the position parameter γ. The thick dotted line is the numerical prediction for D/D_0.

tions from the Stokes-Einstein law, one should find that D/D_0 is a continuous function of γ. We show in Fig. 4 that all the measurements lie indeed on a simple function of γ. For $\gamma > 5$, only a small deviation is noted. D/D_0 drops from 1 to $\frac{1}{3}$ when γ decreases from 5 to 1. For $\gamma < 1$, D/D_0 stays constant and equal to $\frac{1}{3}$.

Let us try to understand Fig. 4 on physical grounds. Light beads are on average far from both walls, have a large value of γ, and the ratio D/D_0 tends to 1, as expected. As the bead approaches the bottom wall, γ decreases. The effect on the diffusivity appears sharply for values of γ around 5, and the ratio D/D_0 drops abruptly when γ becomes smaller. Note that $\gamma \approx 5$ means that the bead is on average three diameters away from the wall: this is when corrections to the Stokes law become noticeable. When the bead is very close to the bottom wall ($\gamma \ll 1$), D/D_0 saturates to a nonzero value, close to $\frac{1}{3}$. It means that the effective viscosity does not diverge as the bead comes in contact with the wall: the bead may indeed move parallel to the plate by simply rolling and pushing the fluid around the contact point. We expect, however, this argument to breakdown when the sample is thin enough that the bead is almost in contract with both plates, preventing it from rolling.

In conclusion, the experiment shows that one can define a position parameter γ such that D/D_0 is a continuous function of it. For values of γ above 5, D is close to the bulk value D_0. As γ decreases, D drops towards $D_0/3$. The transition between these two regimes is characterized by the value of the Boltzmann length scale L with respect to the sample thickness t and the bead radius r. When L is larger than t, D is essentially equal to D_0. When L is smaller than r, the bead sediments to the bottom plate and D is equal to $D_0/3$.

III. NUMERICAL RESULTS

In this section, we review the analytical expressions for the diffusion coefficients $D_\parallel$ and $D_\perp$ for motions parallel and perpendicular to the glass plates. Since we did not record the vertical displacements of the bead, we average $D_\parallel$ over the vertical axis. We compare the numerical results with the experimental values. We then discuss the generalization of Fick's law when the diffusivity is spatially varying.

A. Wall effect on diffusion

The hydrodynamic interactions between a bead of radius r at a distance z from a wall can be expressed in terms of a position-dependent friction tensor η [8]. In the referential frame defined in Fig. 1, the tensor η is diagonal and the drag force experienced by a particle of velocity v is

$$\begin{bmatrix} F_x \\ F_y \\ F_z \end{bmatrix} = -6\pi r \begin{bmatrix} \eta_x & 0 & 0 \\ 0 & \eta_y & 0 \\ 0 & 0 & \eta_z \end{bmatrix} \begin{bmatrix} v_x \\ v_y \\ v_z \end{bmatrix}, \tag{7}$$

with

$$\eta_x = \eta_y \approx \eta_0 [1 - \tfrac{9}{16}(r/z) + \tfrac{1}{8}(r/z)^3 - \tfrac{45}{256}(r/z)^4 - \tfrac{1}{16}(r/z)^5]^{-1} \tag{8}$$

and

$$\eta_z = \eta_0 \tfrac{4}{3} \sinh\alpha \sum_{n=1}^{\infty} \frac{n(n+1)}{(2n-1)(2n+3)} \left[\frac{2\sinh(2n+1)\alpha + (2n+1)\sinh 2\alpha}{4\sinh^2(n+1/2)\alpha - (2n+1)^2 \sinh^2\alpha} - 1 \right], \tag{9}$$

where

$$\alpha = \cosh^{-1}(z/r) .$$

The expression for η_z is exact [23–25] and the one for η_x and η_y is only approximate to order $(r/z)^5$.

For two walls distant by t, we assume that we can add the deviations of η to η_0 from each wall [2]. Denoting by the superscripts b and t the bottom and top walls,

$$\eta_{x,y,z} = \eta^b_{x,y,z}\left[\frac{z}{r}\right] + \eta^t_{x,y,z}\left[\frac{t-z}{r}\right] - \eta_0 , \tag{10}$$

where z is the distance between the bottom plate and the center of mass of the bead.

We define the diffusivity tensor as

$$\mathbf{D}=k_BT/6\pi r\eta=\begin{bmatrix} k_BT/6\pi\eta_x r & 0 & 0 \\ 0 & k_BT/6\pi\eta_y r & 0 \\ 0 & 0 & k_BT/6\pi\eta_z r \end{bmatrix} . \tag{11}$$

We now have two different diffusion coefficients: one related to motions parallel to the glass plates ($D_\parallel=D_x=D_y$) and the other to motions orthogonal to the glass plates ($D_\perp=D_z$).

B. Vertical average

Let us first recall the experimental procedure used to extract the diffusion coefficient D: we average over many trajectories the square of the bead horizontal excursions as a function of time. It is equivalent to the following: we fix a time τ, and choose a bead in the sample. The probability for the bead to be at the initial altitude z is $P_b(z)$. After a time τ, the square of the bead horizontal displacement is measured. It is on average equal to R^2, a function of z and τ. Since we do not select the initial vertical position of the bead, the average horizontal displacement that we measure is then

$$\langle R^2\rangle=\int_0^t R^2(z)P_B(z)dz . \tag{12}$$

We then plot $\langle R^2\rangle$ as a function of τ (see Fig. 3) and the diffusion coefficient D is defined as the slope of the linear fit divided by 4.

If the bead was confined in its initial horizontal plane during time τ, R^2 would be equal to $4D_\parallel(z)\tau$ and the diffusion coefficient would be equal to $\int_0^t D_\parallel(z)P_B(z)dz$. This expression does not agree with the experimental values. However, the bead moves vertically as well as horizontally, and during the time τ explores vertical regions of different horizontal diffusivities. R^2 is thus given by

$$R^2(z,\tau)=4\int_{z-\delta}^{z+\delta} D_\parallel(\zeta)P_B^\delta(\zeta)d\zeta , \tag{13}$$

where $\delta=\frac{1}{2}\sqrt{2D_\perp(z)\tau}$, and where $P_B^\delta(\zeta)$ is the Boltzmann distribution normalized to 1 on a vertical interval of width 2δ. In other words, the bead explores on average during the time τ a vertical slice of thickness 2δ. The measured horizontal displacement is then the vertical average from $(z-\delta)$ to $(z+\delta)$ of $4D_\parallel(z)\tau$, weighted by the Boltzmann distribution normalized to 1 on this interval. Putting back R^2 from Eq. (13) in Eq. (12) gives for the effective diffusion coefficient D

$$D=\int_0^t P_B(z)\left\{\int_{z-\delta}^{z+\delta} D_\parallel(\zeta)P_B^\delta(\zeta)d\zeta\right\}dz . \tag{14}$$

Since δ depends on the observation time τ, D is going to depend also on τ. However, D is only weakly dependent on time: what counts is the ratio of the vertical excursions to the horizontal ones. In our experiment, where the lower limit on τ is such that the bead moves by at least a fraction of its diameter, this dependence does not show up when plotting $\langle R^2\rangle$ as a function of time (see Fig. 3). We also checked numerically that the variation in D when varying τ in our experimental range did not exceed 10%. The values of D/D_0 (theor) reported in the table are computed from Eq. (14) by taking, for each sample a time τ during which the bead would move along any axis by a radius r in the absence of walls [$\tau=(r^2/2D_0)$]. These values are shown in Fig. 4 by the thick dotted line.

C. $\vec{J}=-\mathrm{grad}(DP)$ or $\vec{J}=-D\,\mathrm{grad}P$

Because the diffusion coefficient D is spatially varying, one might ask what is the generalization of Fick's law: $\vec{J}=-\mathrm{grad}(DP)$ or $\vec{J}=-D\,\mathrm{grad}P$ [26–29]? $\vec{J}$ is the diffusion current and P is the probability distribution. Note that choosing for P the usual Boltzmann distribution $P_B(z)$ in Eq. (13) and Eq. (14) implies that the diffusion current is written as $\vec{J}=-D\,\mathrm{grad}P$. Choosing $\vec{J}=-\mathrm{grad}(DP)$ leads to a different density profile equal to $(A/D_\perp)P_B$, where A is a normalization factor. The values of the diffusion coefficient estimated by taking this density profile in Eq. (13) and Eq. (14) do not agree with the experimental values. Also, the physical mechanism underlying the spatial dependence of the diffusivity is, in our case, a hydrodynamic kinetic effect, and cannot change the Boltzmann equilibrium distribution [26,30]. Only a real potential can affect the equilibrium distribution. The correct generalization of Fick's law in our case is $\vec{J}=-D\,\mathrm{grad}P$.

IV. CONCLUSION

From microscopic tracking of spherical particles confined between two glass walls, the diffusivity parallel to the glass plates is obtained. Deviations of the diffusivity D from the bulk value D_0 given by the Stokes-Einstein law are characterized by a dimensionless position parameter γ. The heavier the bead and the smaller the distance between the two glass plates, the bigger the deviation. Values of the ratio D/D_0 as small as $\frac{1}{3}$ are observed. Comparisons with numerical estimates show that the correct generalization of Fick's law is, in our case, $\vec{J}=-D\,\mathrm{grad}P$.

ACKNOWLEDGMENTS

It is a pleasure to thank D. Sornette, J. Lebowitz, and P. Nozières for pointing out to us some essential thermodynamics principles.

[1] A. Einstein, Ann. Phys. (N.Y.) **17**, 549 (1905).
[2] M. I. M. Feitosa and O. N. Mesquita, Phys. Rev. A **44**, 6677 (1991).
[3] N. Garnier and N. Otsrowsky, J. Phys. II **1**, 1221 (1991).
[4] K. H. Lan, N. Ostrowsky, and D. Sornette, Phys. Rev. Lett. **57**, 17 (1986).
[5] G. K. Batchelor, J. Fluid Mech. **74**, 1 (1976).
[6] D. L. Ermak and J. A. McCammon, J. Chem. Phys. **69**, 1352 (1978).
[7] J. A. Hogdon and F. H. Stillinger, Phys. Rev. E **48**, 207 (1993).
[8] H. Faxen, Ark. Mat. Astron. Fys. **18**, 1 (1924).
[9] Bangs Laboratories, Inc., Carmel, IN.
[10] The water was purified by a Hydro Pure Water System from Hydro, Inc., Triangle Research Park, NC.
[11] Tungsten wires from California Fine Wires Company, Grover City, CA.
[12] $75\times50\times1$ mm^3 precleaned microscope slides from Corning Glass Works, Inc., Corning, NY.
[13] $22\times22\times0.05$ mm^3 coverslips number 0 from Fisher Scientific Inc., Pittsburgh, PA.
[14] Simco Topgun from Simco, Inc., Hatfield, PA.
[15] Five minutes fast epoxy from Devcon Corp., Danvers, MA.
[16] IMT-2 from Olympus, Inc., Lake Success, NY.
[17] Olympus SP Plan 100.
[18] TI-24 CCD camera from NEC Electronics, Inc., Mountainview, CA.
[19] Olympus NFK 2.5× Long Distance and 6.7× Long Distance.
[20] MacIIci from Apple Computers, Inc., Cupertino, CA.
[21] H. Brenner, Chem. Eng. Sci. **16**, 242 (1961).
[22] *Lettre au Chevalier Jean Pringle,* B. Franklin, May 1768, London.
[23] A. T. Clark, M. Lal, and G. M. Gibson, Far. Discuss. Chem. Soc. **83**, 179 (1987).
[24] M. D. A. Cooley and M. E. O'Neill, Mathematika **16**, 37 (1969).
[25] A. J. Goldman, R. G. Cox, and H. Brenner, Chem. Eng. Sci. **22**, 637 (1967).
[26] M. J. Schnitzer, Phys. Rev. E **48**, 2553 (1993).
[27] R. Landauer and J. W. F. Woo, in *Synergetics,* edited by H. Haken (Springer-Verlag, Stuttgart, 1973).
[28] R. Landauer, Helv. Phys. Acta **56**, 847 (1983).
[29] N. G. van Kampen, *Stochastic Processes in Physics and Chemistry* (North-Holland, New York, 1981), p. 237.
[30] J. Lebowitz (private communication).

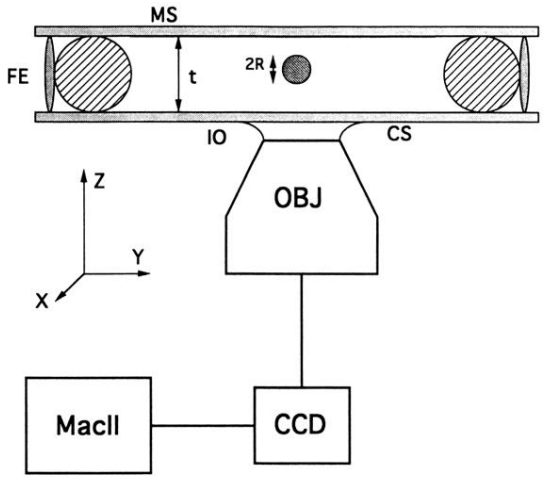

FIG. 1. The experimental setup: beads of diameter $2r$ are suspended in water between a microscope slide (MS) and a cover slip (CS), separated by wires of diameter t. The cell is sealed with fast epoxy (FE). The objective (OBJ) is coupled to the sample by optically index matched immersion oil (IO). The CCD camera digitizes the image which is transmitted to a MacII computer.